Genome-Wide Profiling and Clinical Significance of Alternative Splicing Events in Glioblastoma

Xiufang Ren
Shengjing Hospital of China Medical University
Tianqi Liu
China Medical University Hospital
Xin Chen
China Medical University Hospital
Gefei Guan
China Medical University Hospital
Cunyi Zou
China Medical University Hospital
Qing Guo
China Medical University Hospital
Peng Cheng
China Medical University Hospital
Xiaoyan Xu
China Medical University
Wen Cheng
China Medical University Hospital
Chen Zhu
China Medical University Hospital
Anhua Wu (ahwu@cmu.edu.cn)
China Medical University Hospital

Research

Keywords: glioblastoma, alternative splicing, mesenchymal, immune microenvironment

Posted Date: July 6th, 2020

DOI: https://doi.org/10.21203/rs.3.rs-39549/v1

Abstract

Aims: The purpose of this study was to depict alternative splicing (AS) profiles in GBM and identify their clinical significance in the progression of GBM.

Materials and Methods: RNA sequence data and clinical information were downloaded from The Cancer Genome Atlas portal (https://portal.gdc.cancer.gov/projects). Genome-wide alternative splicing events were obtained using SpliceSeq tool. Analyses were performed using GraphPad Prism 7 and R software.

Key findings: Univariate Cox analysis identified 2406 AS events with prognostic significance. We built an interaction network based on these survival-related AS events. Unsupervised clustering analysis showed that patients in cluster 2 had a better prognosis than those in other clusters. The prognostic splicing factors and AS events were used to generate a splicing network. Seven prognostic signatures, developed based on the top three survival-related AS events, predicted the survival risk and may serve as independent indicators of unfavorable prognosis. Among these risk signatures, only the alternate promoter (AP) signature was upregulated in the mesenchymal subtype, which is characterized by a complex immune microenvironment. A high AP risk score indicated an overloaded local immune response and enriched immune cell infiltration, which may accelerate the progression of GBM.

Significance: AS-related signatures may serve as predictors of prognosis as well as provide treatment targets and guidance for GBM patients.

1. Introduction

Glioblastoma (GBM) is the most common and lethal type of tumor of the central nervous system [1]. Despite advances in treatment options, the median survival of patients with GBM is approximately 14 months. Recent studies highlighted immune disorders as key drivers promoting GBM malignancy. Previous work from our group showed that an overloaded immune response and disorganized immune microenvironment contribute to poor outcomes and resistance to therapy in GBM [2–4].

Alternative splicing (AS) is a common post-transcriptional regulatory mechanism that promotes protein diversity through differential pre-mRNA splicing. More than 90% of multi-exon genes undergo AS [5]. Recent evidence supports a relationship between AS and the occurrence or progression of cancer [6]. In addition, unbalanced expression of splicing variants or failure to properly express the correct isoform is a hallmark of cancer [7, 8]. However, the role of AS in GBM progression remains elusive

Here, we collected splicing data of 157 GBM samples from the SpliceSeq database. We conducted a systematic analysis by merging the AS data with clinical information and the expression matrix. In addition, we developed seven prognostic signatures based on the top three survival-related AS events, and identified a mesenchymal-specific and immune-related AS signature with prognostic significance. This study is the first to examine the relationship between AS and the malignant biological features of

GBM in a large cohort. The results revealed the clinical value of different AS events, and may provide a new prognostic indicator and potential targets for immune therapy in GBM.

2. Material And Methods

2.1 AS data curation process

RNA sequence data and clinical information were downloaded from The Cancer Genome Atlas (TCGA) portal (https://portal.gdc.cancer.gov/projects). The genome-wide AS events were obtained using SpliceSeq tool, a java application that was used to analyze the AS profiles and mRNA splicing patterns of TCGA samples [9]. The percent spliced in (PSI) value was used to quantify AS events in GBM and ranged from 0 to 1. Seven types of AS events were analyzed: alternate acceptor site (AA), alternate donor site (AD), alternate promoter (AP), alternate terminator (AT), exon skip (ES), mutually exclusive exons (ME), and retained intron (RI).

2.2 Survival analysis

Univariate Cox regression analysis was performed to identify the prognostic AS events and splicing factors. Multivariate Cox regression analysis was used to identify independent prognostic factors. The Kaplan-Meier survival curve was used to analyze the prognostic differences between groups. Receiver operating characteristic (ROC) curves were generated to assess the survival prediction accuracy.

Patients with a survival time of < 30 days were excluded.

2.3 Functional enrichment analysis

The Limma R package was used to screen out differentially expressed genes based on an absolute fold change value >1.5 and adjusted p value < 0.05. Gene Ontology (GO) and Kyoto Encyclopedia of Genes and Genomes (KEGG) analyses were performed using the ClueGo plugin of Cytoscape and the Database for Annotation, Visualization, and Integrated Discovery (DAVID) website [10-12]. Gene set enrichment analyses (GSEA) were performed to estimate the enrichment of specific gene sets [13]. Principal components analysis (PCA) was used to identify the expression patterns of different groups under a specific gene set background.

2.4 Tumor microenvironment analysis

Tumor purity was estimated as described previously and calculated according to the formula reported by Yoshihara [14]. The estimation of eight types of immune cells and two prominent stromal cells was performed using Microenvironment Cell Populations-counter (MCP-counter) [15].

2.5 AS-related network, cluster, and predictive signature construction

The interaction network of survival-associated AS genes in GBM was generated by Reactome FI plugin of Cytoscape to explore the potential interactions among survival-related AS events and identify the hub

genes. Splicing factor information was downloaded from the SpliceAid2 database (http://www.introni.it/splicing.html). The correlation network between the survival-related splicing factors and the corresponding AS events was visualized by Cytoscape. The cluster analyses based on the survival-related AS events were performed by consensus unsupervised analysis according to the ClusterProfiler R package [16]. Seven predictive signatures were established with different types of AS events according to the results of univariate Cox regression analysis. For each AS event, the top three survival-related events with a PSI value > 0.5 were identified to construct the predictive model.

2.6 Statistical analysis

UpSet plot was used to visualize the intersections between the seven types of prognostic AS events in GBM using UpSet R package [17]. The correlation between two parameters was determined by Spearman correlation analysis. All statistical analyses were performed using GraphPad Prism 7 and R software. A two sided P value <0.05 was considered statistically significant.

3. Results

3.1 Overview of AS events profiling in GBM

To profile the AS events in GBM, seven types of AS events present in GBM patients were analyzed (Figure. 1A). A total of 45610 AS events from 21134 genes were detected, which indicated that one gene was associated with approximately two AS events. We detected 3827 AA events in 2684 genes, 3269 AD events in 2269 genes, 8686 AP events in 3476 genes, 8456 AT events in 3696 genes, 18360 ES events in 6933 genes, 184

ME events in 180 genes, and 2828 RI events in 1896 genes. ES events were the most frequently detected, accounting for nearly half of the total AS events. The frequency of ME events was lower than that of other types of AS events (Figure. 1B).

3.2 Identification of prognostic AS events in GBM

The relationship between AS events and the prognosis of GBM patients was examined by univariate Cox regression analysis. Among the 45610 AS events, 1643 were identified as survival-associated AS events ($P < 0.05$). Because one gene might have more than one event, we visualized the intersecting survival-associated AS events using UpSet PlotR. The results showed that one gene could have up to three types of AS events significantly associated with GBM survival (Figure. 1C). Construction of a gene network by Reactome of Cytoscape including the 300 most significant survival-associated genes identified several genes, such as UBC, STAT3, and FYN, that could serve as the hub genes in the network. The pathways mediated by these genes may play critical roles in regulating the AS network (Figure. 1D).

3.3 Cluster analysis based on prognostic AS events in GBM

To better predict the prognosis of GBM patients based on the scale of AS events, consensus unsupervised clustering was performed based on the 1643 prognostic AS events. We found that the

optimal number of clusters was five (Figure. 2A). GBM patients were assigned into five clusters as follows: cluster 1 (n = 100, 62.5%), cluster 2 (n = 24, 15%), cluster 3 (n = 26, 16.25%), cluster 4 (n = 7, 4.375%), and cluster 5 (n = 3, 1.875%). Because of the small number of patients in clusters 4 and 5, we performed survival analysis including clusters 1–3. Patients in cluster 2 showed significantly better survival than those in the other two clusters (Figure. 2B). The results of proportional analysis to characterize the molecular subtype of AS clusters suggested that cluster 2 was robustly correlated with the proneural subtype (Figure. 2C, D), which may be related to the better prognosis of cluster 2. However, assessing the prognosis of the other four clusters was challenging.

3.4 Regulatory network between prognostic splicing factors and prognostic AS events

AS profiles are regulated by several splicing factors that affect exon selection and splicing site choice by binding to pre-mRNAs [18]. To explore the correlation between the prognostic AS events and known splicing factors, data on splicing factors was obtained from SpliceAid2 and TCGA databases. Univariate Cox regression analysis showed that only five splicing factors (KHDRBS2, TIA1, TIAL1, ZRANB2, and PTBP2) were significantly associated with overall survival (Supplementary Table S1). The relationship between the expression of the five splicing factors and the PSI value of prognostic AS events was determined to build a splicing regulatory network (Figure. 2E). The splicing regulatory network identified 57 survival-associated AS events, including 39 unfavorable events (orange dots) and 18 favorable events (green dots), that were significantly correlated with the five splicing factors (purple dots). Most of the favorable AS events were positively correlated with splicing factors (green lines), whereas most unfavorable AS events had a negative correlation with splicing factors. For example, ZRANB2, one the most significant survival-related splicing factors, was positively correlated with the ERCC5 RI event, whereas it exhibited a significant negative correlation with C19orf53 of AP, which were favorable and adverse prognostic AS events, respectively (Figure. 2F, G). Kaplan-Meier survival analyses indicated that ZRANB2 was marginally correlated with survival regardless of the cutoff value, such as the tripartite point and the quarter point (Figure. 2H–J). The remaining four splicing factors showed similar relationships (data not shown). These data indicate that the splicing factors were not accurate predictors of survival in GBM patients.

3.5 Development of an individualized prognostic AS signature

Because a signature is more accurate for predicting overall survival than a single event, individual signatures were constructed for seven AS events to improve prognosis prediction in GBM. For each type of AS event, the top three prognostic AS events were identified according to the univariate Cox regression results (Figure. 3A–G). The results of the analysis of the 21 AS events are summarized in Table 1. The AS signatures were calculated as follows: risk score = (lnHR of the top AS event × PSI value of the top AS event + lnHR of the top two AS events × PSI value of the top two AS events + lnHR of the top three AS events × PSI value of the top three AS events). We further combined the seven signatures into one model and calculated the risk score as follows = (lnHR of AA × AA score + lnHR of AD × AD score + lnHR of AP × AP score + lnHR of AT × AT score + lnHR of ES × ES score + lnHR of ME × ME score + lnHR of RI × RI score). The median risk score was used as the cutoff to divide the patients into high or low risk groups. The eight predictive models indicated that the survival status of the high-risk groups was worse than that of the corresponding low risk groups (Figure. 3A–G).

Table 1
Top 3 survival related events of seven types of AS.

AS Events_ID	Gene Symbol	Type	HR	Adj P value	LnHR
ID_19897	CHD4	AA	0.0381	0.000849	-3.266
ID_30617	DMXL2	AA	0.094	0.0025	-2.364
ID_64840	USP19	AA	0.0457	0.0086	-3.085
ID_48995	ZNF302	AD	0.0176	0.00027	-4.04
ID_41811	TMUB2	AD	0.0897	0.0044	-2.41
ID_14562	SERGEF	AD	8.444	0.00526	2.133
ID_76351	TMEM63B	AP	0.0253	0.000317	-3.679
ID_3657	DDAH1	AP	40.938	0.000557	3.712
ID_74448	MAT2B	AP	0.0135	0.000933	-4.307
ID_78181	SYNE1	AT	0.0035	0.00032	-5.642
ID_44016	CCDC40	AT	88.91	0.0016	4.488
ID_72688	RPS23	AT	0.0121	0.0019	-4.413
ID_29531	C14orf2	ES	6.337	0.0001	1.847
ID_46873	HSD11B1L	ES	36.32	0.00016	3.592
ID_127358	MRPS28	ES	17.127	0.00035	2.841
ID_10258	TTC13	ME	0.211	0.0133	-1.554
ID_100824	RPE	ME	0.248	0.0167	-1.394
ID_35718	CLN3	ME	26.391	0.0199	3.273
ID_10337	COA6	RI	0.0616	0.0018	-2.787
ID_85333	SLC45A4	RI	0.108	0.0035	-2.222
ID_69370	HOPX	RI	7.352	0.0042	1.995

Abbreviations: AS, alternative splicing; AA, Alternate Acceptor Site; AD, Alternate Donor Site; AP, Alternate Promoter; AT, Alternate Terminator; ES, Exon Skip; ME, Mutually Exclusive Exons; RI, Retained Intron; HR, hazard ratio.

Kaplan-Meier survival analyses according to the eight predictive signatures showed that survival time was considerably shorter for high risk patients than for low risk patients (Figure. 4A–H). ROC curves for 1-year survival were drawn to estimate the specificity and sensitivity of each signature. The results showed that the AS signatures had good predictive ability, and the combined model including all signatures had a better predictive accuracy than each individual signature (Figure. 4I). The potential of the AS-associated signatures as independent predictive factors was assessed by univariate and multivariate Cox analyses. Classical survival-related clinical parameters were identified in the univariate Cox regression analysis (Supplementary Table S2). The results of multivariate Cox analyses indicated that the eight signatures were independently correlated with GBM survival after adjusting for age, IDH1 mutation status, MGMT methylation status, chemotherapy, and radiotherapy (Table 2). These findings suggest that AS-associated signatures can predict the survival of GBM patients in a stable and independent manner.

Table 2
Cox Regression Analysis of TCGA RNA seq database.

(Adjusted by Age,IDH1,MGMT,Chemotherapy and Radiotherapy)		
Multi-Variate Regression		
Variable	HR	P value
AA signature	1.939	0.017
(High RiskScore VS Low RiskScore)		
AD signature	1.632	0.048
(High RiskScore VS Low RiskScore)		
AP signature	2.332	0.00015
(High RiskScore VS Low RiskScore)		
AT signature	1.725	0.0409
(High RiskScore VS Low RiskScore)		
ES signature	1.736	0.0033
(High RiskScore VS Low RiskScore)		
ME signature	3.299	5.50E-03
(High RiskScore VS Low RiskScore)		
RI signature	2.895	3.20E-04
(High RiskScore VS Low RiskScore)		
ALL signature	1.979	1.70E-07
(High RiskScore VS Low RiskScore)		

Abbreviations: TCGA, The Cancer Genome Atlas; AS, alternative splicing; AA, Alternate Acceptor Site; AD, Alternate Donor Site; AP, Alternate Promoter; AT, Alternate Terminator; ES, Exon Skip; ME, Mutually Exclusive Exons; RI, Retained Intron; HR, hazard ratio.

3.6 The AP signature was identified as an immune relevant signature

To assess the association between the seven predictive signatures and GBM molecular subtypes, the risk scores for four molecular subtypes were analyzed. The AP risk score was significantly increased in the mesenchymal subtype (Figure. 5A), which is an immune relevant subtype [19]. PCA based on immune related genes showed that the distribution pattern of the mesenchymal samples was different from that of non-mesenchymal samples, suggesting that the immune status of the mesenchymal subtype differed from that the other three subtypes (Figure. 5B). GO and KEGG analyses of significantly upregulated genes in the mesenchymal subtype were performed in the DAVID website, and the enrichment results showed that the most relevant biological processes were immune-related terms such as immune response and leukocyte chemotaxis (Figure. 5C).

The close association between the AP risk score and the mesenchymal subtype indicated that the AP signature could be considered as an immune-related AS signature. To validate this hypothesis, differentially expressed genes between high AP risk and low AP risk patients were identified, and the ClueGo plugin of Cytoscape was used to analyze the functional enrichment. The results showed that the most relevant biological processes were immune response and immune cell chemotaxis (Figure. 6A). Moreover, we depicted the most common somatic mutation events in GBM stratified by AP score (Figure. 6B). The results showed that the low AP score group occupied more IDH1 mutation, which was another indication of that AP score involved with immune response and microenvironment (Fig. 6C). These findings were confirmed by GSEA (Figure. 6D–F). Consistent with our previous study [4], tumor purity was a key factor affecting the prognosis of glioma patients. To explore the effect of the AP risk on the composition of the immune microenvironment, tumor purity was assessed for each patient, as well as the

enrichment score of several hub non-tumor cells. Correlation analysis showed a significant negative correlation between the AP risk score and GBM purity (Figure. 6G). Analysis of the correlations between AP risk and the scores of eight hub non-tumor cells suggested that neutrophils were the most relevant components of the microenvironment involved in AP risk (Figure. 6H). These findings indicated that the AP signature may predict the prognosis of GBM through its effect on the immune response and the composition of the immune microenvironment.

4. Discussion

Increasing evidence supports the contribution of aberrant AS events or splicing factors to the malignant progression of glioma. AS can modulate transcriptional activity in glioma [20], and AS of telomerase reverse transcriptase is modulated by CX-5461 in glioma [21]. Splicing factors are also involved in glioma progression; SRSF1 is a splicing factor that promotes gliomagenesis via oncogenic splice-switching of MYO1B [22]. Studies suggest that apoptotic cell-derived extracellular vesicles promote GBM malignancy by mediating the intracellular transfer of splicing factors [23]. AS contributes to the variability of isoforms, which may play different roles in the progression of GBM [24, 25]. Therefore, it is of great importance to elucidate the ambiguous functions of AS events and to determine the levels of splicing factors in GBM. However, comprehensive genome-wide profiling or analysis of the clinical significance of AS events in a large glioma cohort is limited, especially in GBM patients. In this study, profiling of AS events was performed in a large cohort of GBM patients, and AS related signatures were established to predict survival outcomes.

The present AS related genome-wide analysis identified seven AS modes in GBM patients, and showed that one gene was generally associated with two AS events, which is consistent with data in other tumors [26, 27]. ES events accounted for approximately 50% of all AS events, indicating that they may be the most important AS events contributing to the malignancy of GBM; however, further functional experiments are necessary to confirm these findings. To identify AS events with prognostic value that may serve as promising targets, gene network analysis by Cytoscape was performed including the top 300 survival related events, and several AS-related genes such as UBC, STAT3, and FYN were identified as hub genes. Then, we attempted to perform unsupervised analysis, which is considered as a better method to predict survival based on AS events [28]. However, the results showed that only one cluster was associated with survival status, which accounted for a small proportion of GBM patients. The predictive ability of the cluster was limited, and the majority of GBM patients could not be distinguished. Because splicing factors play critical roles in malignant progression [29, 30], we constructed a splicing factor related regulatory network. However, the predictive ability was low even for survival-associated spicing factors.

Considering stable traits and the applicability of risk signatures [26–28, 31], we developed seven prognostic signatures based on the top three survival-related AS events. The results showed that all the AS-related signatures could significantly distinguish the survival status and serve as independent indicators of unfavorable prognosis. Studies indicate that the central nervous system is not immune-privileged [32]. Moreover, previous studies from our group demonstrated that the overloaded immune

response as well as the disorganized immune microenvironment contribute to the malignancy of GBM [2–4]. There is limited data on the influence of AS events on immune regulation. In the present study, we showed that STAT3 and FYN, which are involved in immune regulation, occupy hub positions among the network of survival related AS events [33, 34]. These results supported the existence of a robust correlation between AS and immune responses. Because the molecular subtype of GBM is associated with the immune status, we compared the risk scores for four molecular subtypes. The results showed that only the AP risk score was considerably increased in the mesenchymal subtype, which is the subtype with the most involved immune status and microenvironment [19]. Further biological enrichment analyses confirmed that the AP risk score was associated with an enhanced immune response. Analysis of the immune microenvironment showed that the AP score was negatively correlated with tumor purity, whereas it was positively correlated with several immune components, such as NK cells and neutrophils. In previous work, we identified neutrophils as components of the microenvironment associated with AP risk in glioma. These findings indicate that interfering with AP related events may increase the efficacy of immunotherapy in GBM patients.

5. Conclusion

In this study, we performed genome-wide profiling of AS events and identified AS events with significant prognostic value in GBM patients. We also established AS-related predictive signatures based on different AS modes, and found an association between the AP signature and immune responses. AS-related signatures may have predictive ability and provide useful treatment targets and guidance for GBM patients. One limitation of the study was the lack of validation cohorts. Future studies should focus on functional experiments and on exploring the molecular mechanisms underlying the effect of AP signature-related events on the immune response and microenvironment.

Abbreviations

AS: alternative splicing; GBM: glioblastoma ; TCGA: The Cancer Genome Atlas ; PCA: principal components analysis ; GO: gene ontology; KEGG: Kyoto encyclopedia of genes and genomes; GSEA: gene set enrichment analyses; PSI: percent spliced in; AA: alternate acceptor site; AD: alternate donor site; AP: alternate promoter; AT: alternate terminator; ES: exon skip; ME: mutually exclusive exons; RI: retained intron; ROC: receiver operating characteristic; MCP-counter: microenvironment cell populations-counter

Declarations

Acknowledgements

We thank the members of Dr. Wu AH's laboratory for help with our study.

Author contributions

Conception and design: Ren XF, Cheng W, Wu AH, Zhu C, Liu TQ, Chen X; data download and curation: Zhu C, Guan GF, Liu TQ; methodology: Cheng P. and Xu XY.; data analyses and interpretation: Ren XF, Zhu C, Zou CY, Chen X and Guo Q; manuscript writing and revision: Zhu C, Cheng W and Wu AH. All authors read and approved the final manuscript.

Funding

This work was supported by the National Natural Science Foundation of China [No.81872054] & [No.81872057] & [No.81902546].

Availability of data and materials

The alternative splicing events were obtained using SpliceSeq tool (https://bioinformatics.mdanderson.org/TCGASplice-Seq/). The splicing factors' information was downloaded from the SpliceAid2 database (http://www.introni.it/splicing.html). The gene expression matrix and associated clinical information in this study can be found on TCGA portal (https://portal.gdc.cancer.gov/projects).

Disclosure of conflict of interest

None

Ethics approval and consent to participate

None

References

1. Morgan LL. The epidemiology of glioma in adults: a "state of the science" review. Neuro Oncol. 2015;17:623–4.
2. Cheng W, Ren X, Zhang C, Cai J, Liu Y, Han S, Wu A. Bioinformatic profiling identifies an immune-related risk signature for glioblastoma. Neurology. 2016;86:2226–34.
3. Han S, Zhang C, Li Q, Dong J, Liu Y, Huang Y, Jiang T, Wu A. Tumour-infiltrating CD4(+) and CD8(+) lymphocytes as predictors of clinical outcome in glioma. Br J Cancer. 2014;110:2560–8.
4. Zhang CB, Cheng W, Ren X, Wang Z, Liu X, Li G, Han S, Jiang T, Wu A. Tumor Purity As an Underlying Key Factor in Glioma. Clin Cancer Res. 2017;23:6279–91.
5. Nilsen TW, Graveley BR. Expansion of the eukaryotic proteome by alternative splicing. Nature. 2010;463:457–63.
6. Climente-Gonzalez H, Porta-Pardo E, Godzik A, Eyras E. The Functional Impact of Alternative Splicing in Cancer. Cell Rep. 2017;20:2215–26.
7. Ladomery M. Aberrant alternative splicing is another hallmark of cancer. Int J Cell Biol 2013; 2013: 463786.

8. Oltean S, Bates DO. Hallmarks of alternative splicing in cancer. Oncogene. 2014;33:5311–8.
9. Ryan MC, Cleland J, Kim R, Wong WC, Weinstein JN. SpliceSeq: a resource for analysis and visualization of RNA-Seq data on alternative splicing and its functional impacts. Bioinformatics. 2012;28:2385–7.
10. Bindea G, Mlecnik B, Hackl H, Charoentong P, Tosolini M, Kirilovsky A, Fridman WH, Pages F. Trajanoski Z and Galon J. ClueGO: a Cytoscape plug-in to decipher functionally grouped gene ontology and pathway annotation networks. Bioinformatics. 2009;25:1091–3.
11. Huang da W, Sherman BT, Lempicki RA. Systematic and integrative analysis of large gene lists using DAVID bioinformatics resources. Nat Protoc. 2009;4:44–57.
12. Huang da W, Sherman BT, Lempicki RA. Bioinformatics enrichment tools: paths toward the comprehensive functional analysis of large gene lists. Nucleic Acids Res. 2009;37:1–13.
13. Subramanian A, Tamayo P, Mootha VK, Mukherjee S, Ebert BL, Gillette MA, Paulovich A, Pomeroy SL, Golub TR, Lander ES, Mesirov JP. Gene set enrichment analysis: a knowledge-based approach for interpreting genome-wide expression profiles. Proc Natl Acad Sci U S A. 2005;102:15545–50.
14. Bindea G, Mlecnik B, Tosolini M, Kirilovsky A, Waldner M, Obenauf AC, Angell H, Fredriksen T, Lafontaine L, Berger A, Bruneval P, Fridman WH, Becker C, Pages F, Speicher MR, Trajanoski Z, Galon J. Spatiotemporal dynamics of intratumoral immune cells reveal the immune landscape in human cancer. Immunity. 2013;39:782–95.
15. Becht E, Giraldo NA, Lacroix L, Buttard B, Elarouci N, Petitprez F, Selves J, Laurent-Puig P, Sautes-Fridman C, Fridman WH, de Reynies A. Estimating the population abundance of tissue-infiltrating immune and stromal cell populations using gene expression. Genome Biol. 2016;17:218.
16. Yu G, Wang LG, Han Y, He QY. clusterProfiler: an R package for comparing biological themes among gene clusters. Omics. 2012;16:284–7.
17. Lex A, Gehlenborg N, Strobelt H, Vuillemot R, Pfister H. UpSet: Visualization of Intersecting Sets. IEEE Trans Vis Comput Graph. 2014;20:1983–92.
18. Fredericks AM, Cygan KJ, Brown BA, Fairbrother WG. RNA-Binding Proteins: Splicing Factors and Disease. Biomolecules. 2015;5:893–909.
19. Doucette T, Rao G, Rao A, Shen L, Aldape K, Wei J, Dziurzynski K, Gilbert M, Heimberger AB. Immune heterogeneity of glioblastoma subtypes: extrapolation from the cancer genome atlas. Cancer Immunol Res. 2013;1:112–22.
20. Li J, Wang Y, Meng X, Liang H. Modulation of transcriptional activity in brain lower grade glioma by alternative splicing. PeerJ. 2018;6:e4686.
21. Li G, Shen J, Cao J, Zhou G, Lei T, Sun Y, Gao H, Ding Y, Xu W, Zhan Z, Chen Y, Huang H. Alternative splicing of human telomerase reverse transcriptase in gliomas and its modulation mediated by CX-5461. J Exp Clin Cancer Res. 2018;37:78.
22. Zhou X, Wang R, Li X, Yu L, Hua D, Sun C, Shi C, Luo W, Rao C, Jiang Z, Feng Y, Wang Q, Yu S. Splicing factor SRSF1 promotes gliomagenesis via oncogenic splice-switching of MYO1B. J Clin Invest. 2019;129:676–93.

23. Pavlyukov MS, Yu H, Bastola S, Minata M, Shender VO, Lee Y, Zhang S, Wang J, Komarova S, Wang J, Yamaguchi S, Alsheikh HA, Shi J, Chen D, Mohyeldin A, Kim SH, Shin YJ, Anufrieva K, Evtushenko EG, Antipova NV, Arapidi GP, Govorun V, Pestov NB, Shakhparonov MI, Lee LJ. Nam DH and Nakano I. Apoptotic Cell-Derived Extracellular Vesicles Promote Malignancy of Glioblastoma Via Intercellular Transfer of Splicing Factors. Cancer Cell. 2018;34:119–35.e110.
24. Choi SH, Kim JK, Jeon HY, Eun K, Kim H. OCT4B Isoform Promotes Anchorage-Independent Growth of Glioblastoma Cells. Mol Cells. 2019;42:135–42.
25. Shao Y, Chong W, Liu X, Xu Y, Zhang H, Xu Q, Guo Z, Zhao Y, Zhang M, Ma Y, Gu F. Alternative splicing-derived intersectin1-L and intersectin1-S exert opposite function in glioma progression. Cell Death Dis. 2019;10:431.
26. Zhang D, Duan Y, Cun J, Yang Q. Identification of Prognostic Alternative Splicing Signature in Breast Carcinoma. Front Genet. 2019;10:278.
27. Zong Z, Li H, Yi C, Ying H, Zhu Z, Wang H. Genome-Wide Profiling of Prognostic Alternative Splicing Signature in Colorectal Cancer. Front Oncol. 2018;8:537.
28. Xiong Y, Deng Y, Wang K, Zhou H, Zheng X, Si L, Fu Z. Profiles of alternative splicing in colorectal cancer and their clinical significance: A study based on large-scale sequencing data. EBioMedicine. 2018;36:183–95.
29. Bielli P, Panzeri V. The Splicing Factor PTBP1 Promotes Expression of Oncogenic Splice Variants and Predicts Poor Prognosis in Patients with Non-muscle-Invasive Bladder Cancer. 2018; 24: 5422–5432.
30. Gokmen-Polar Y, Neelamraju Y, Goswami CP, Gu Y, Gu X, Nallamothu G, Vieth E, Janga SC. Splicing factor ESRP1 controls ER-positive breast cancer by altering metabolic pathways. 2019; 20.
31. Shukla S, Evans JR, Malik R, Feng FY, Dhanasekaran SM, Cao X, Chen G, Beer DG, Jiang H, Chinnaiyan AM. Development of a RNA-Seq Based Prognostic Signature in Lung Adenocarcinoma. J Natl Cancer Inst 2017; 109.
32. Wang Q, Hu B, Hu X, Kim H, Squatrito M, Scarpace L, deCarvalho AC, Lyu S, Li P, Li Y, Barthel F, Cho HJ, Lin YH, Satani N, Martinez-Ledesma E, Zheng S, Chang E, Gabriel Sauve CE, Olar A, Lan ZD, Finocchiaro G, Phillips JJ, Berger MS, Gabrusiewicz KR, Wang G, Eskilsson E, Hu J, Mikkelsen T, DePinho RA, Muller F, Heimberger AB, Sulman EP. Nam DH and Verhaak RGW. Tumor Evolution of Glioma-Intrinsic Gene Expression Subtypes Associates with Immunological Changes in the Microenvironment. Cancer Cell. 2018;33:152.
33. Wang Y, Shen Y, Wang S, Shen Q, Zhou X. The role of STAT3 in leading the crosstalk between human cancers and the immune system. Cancer Lett. 2018;415:117–28.
34. Zhang Q, Song X, Su P, Li R, Liu C, Gou M, Wang H, Liu X, Li Q. A novel homolog of protein tyrosine kinase Fyn identified in Lampetra japonica with roles in the immune response. Gene. 2016;579:193–200.

Figures

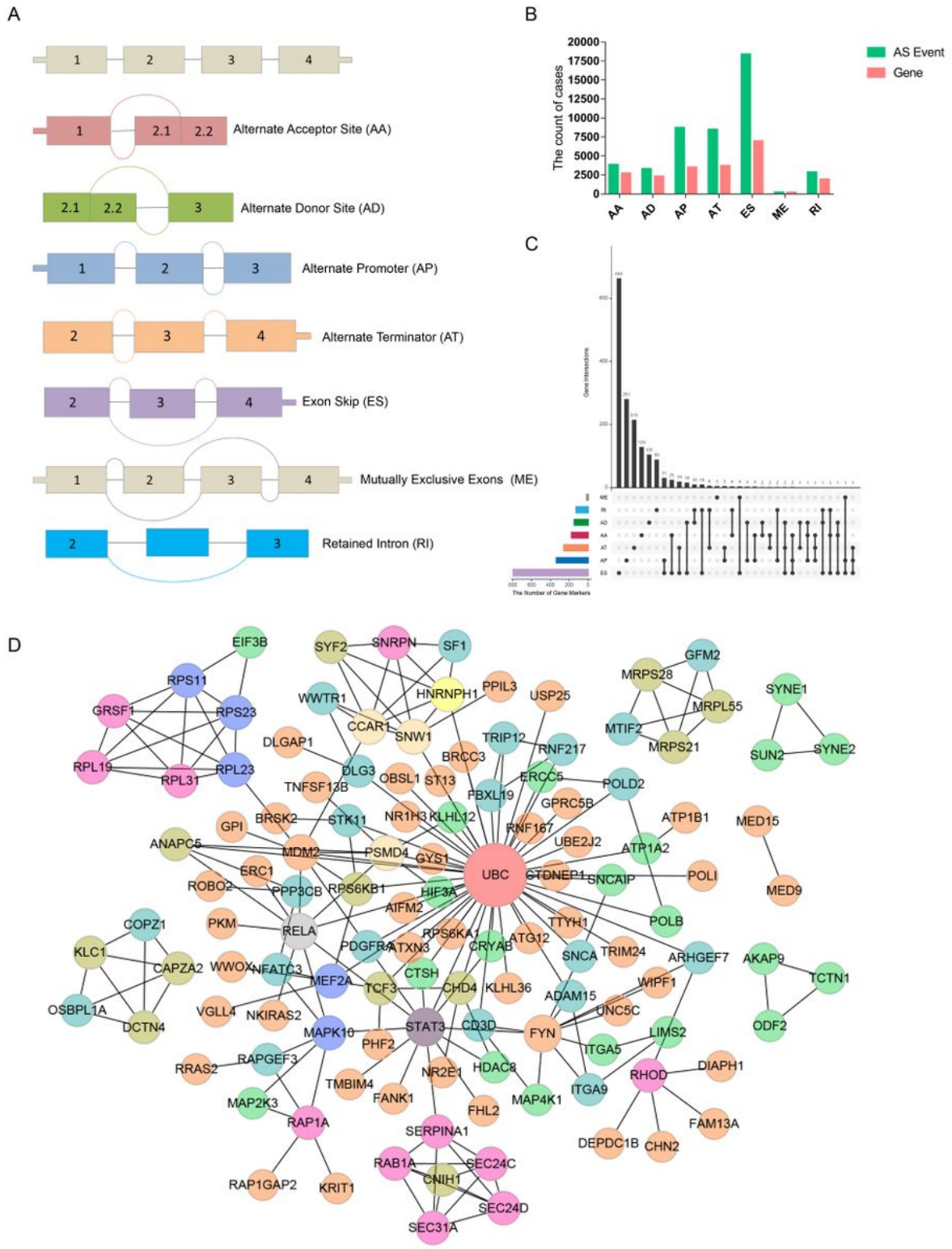

Figure 1

Overview of AS profiling and survival related AS events in GBM. (A) The modes of seven types of AS events. (B) The counts of AS events and involved genes of GBM patients. (C) UpSet plot of interactions among the seven types of survival-related events. (D) Gene network constructed by Reactome of Cytoscape among the 300 most significant survival-associated AS events.

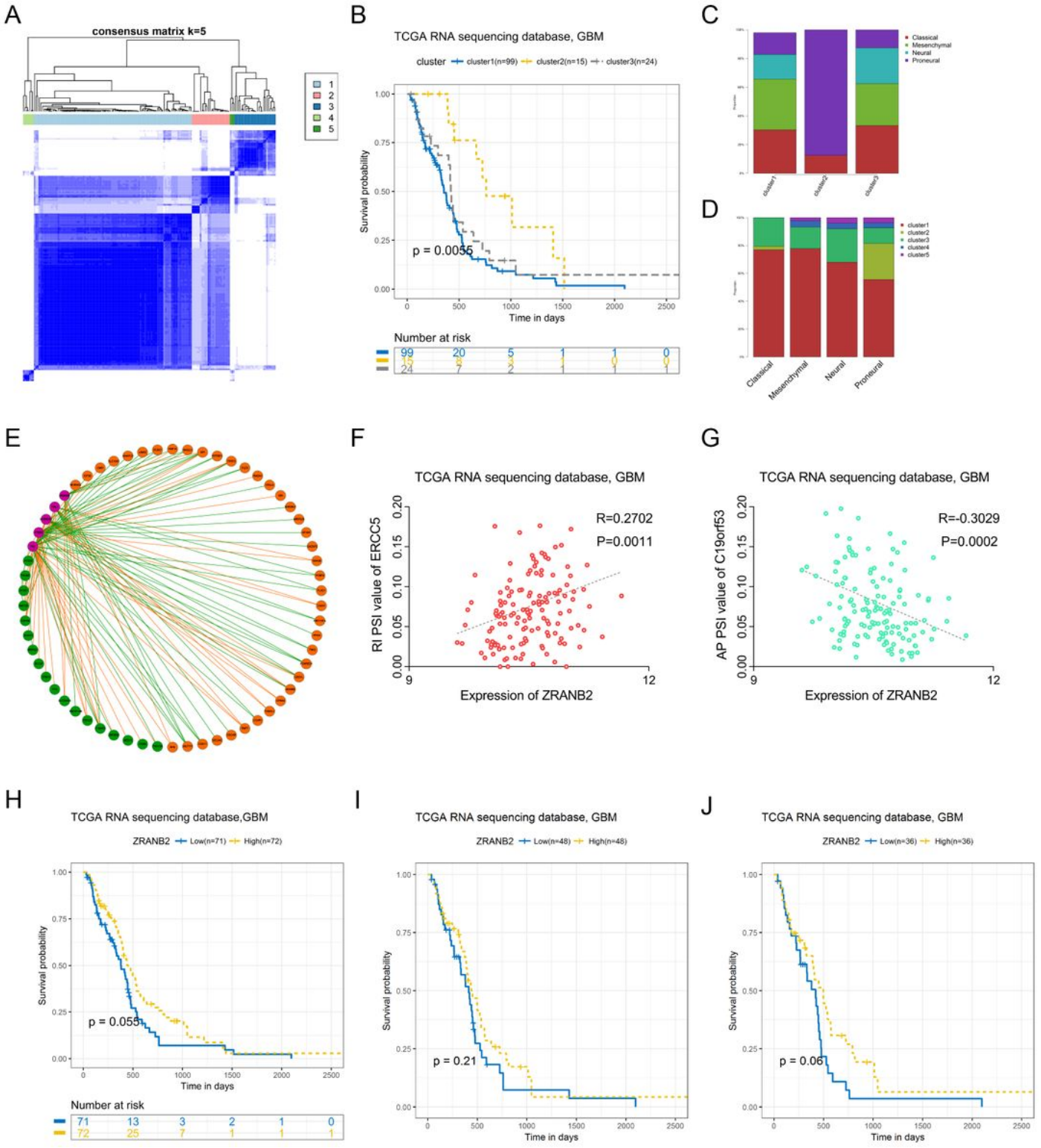

Figure 2

Cluster analysis and construction of splicing factor regulation network in GBM. (A) Five clusters were defined by consensus unsupervised analysis based on the 1643 prognostic AS events. B, Survival analysis among the clusters of GBM patients. (C and D) Cluster 2 was robustly correlated with the proneural subtype of GBM. (E) The potential regulatory network between five prognostic splicing factors and survival-related AS events. (F and G) Correlation analyses between ZRANB2 and two representative

survival-related AS events (ERCC5 of RI event was favorable and C19orf53 AP event was unfavorable). (H–J) Kaplan-Meier survival analyses of ZRANB2 stratified by different cutoff values.

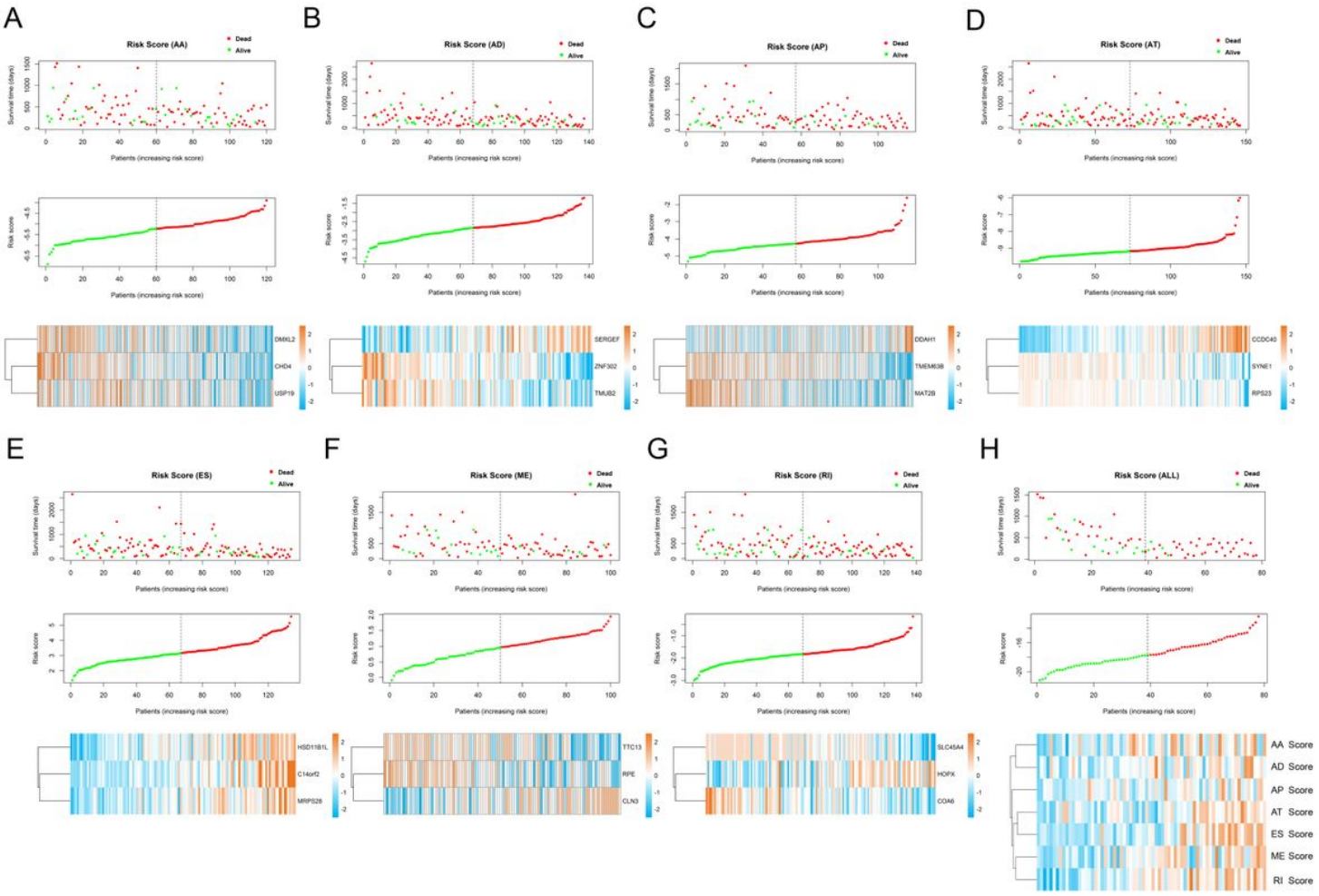

Figure 3

Development of individualized prognostic AS signatures. (A–G) Individual AS related prognostic signatures were established based on the corresponding top three prognostic AS events. (H) Seven types of signatures were combined to construct an integrated prognostic signature (the top part of each assembly drawing represents survival status of GBM patients stratified by risk score; the middle part is the risk score curve of GBM patients; the bottom part exhibits the heatmap of constituting elements).

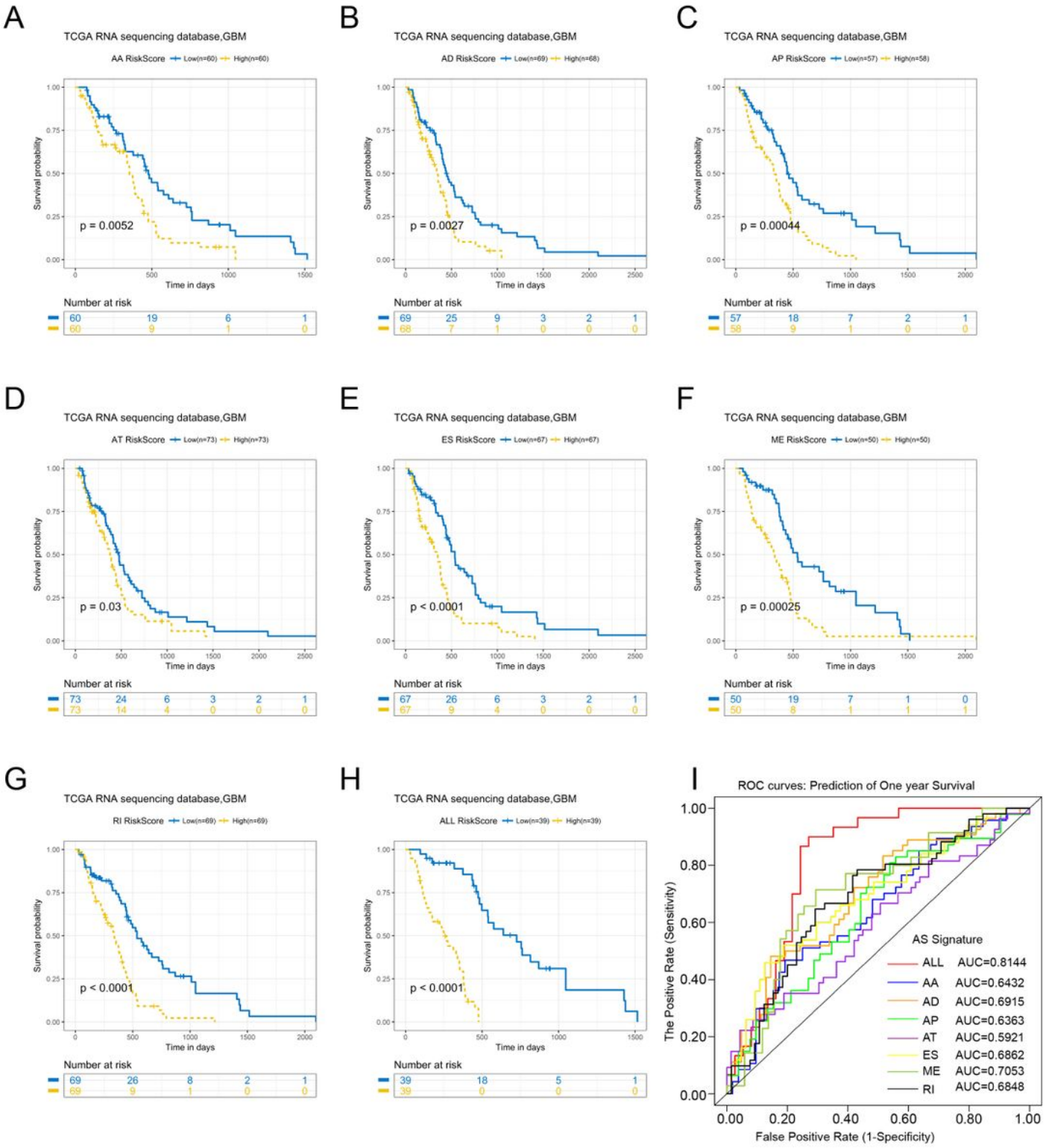

Figure 4

The predictive ability of individualized AS signatures for GBM prognosis. (A–H) Kaplan-Meier survival analyses showed that high risk patients had a lower survival time than low risk patients. ROC curves of 1-year survival were drawn to estimate the specificity and sensitivity of each signature. (I) The combined signature (all signatures) had a better predictive accuracy than each individual signature.

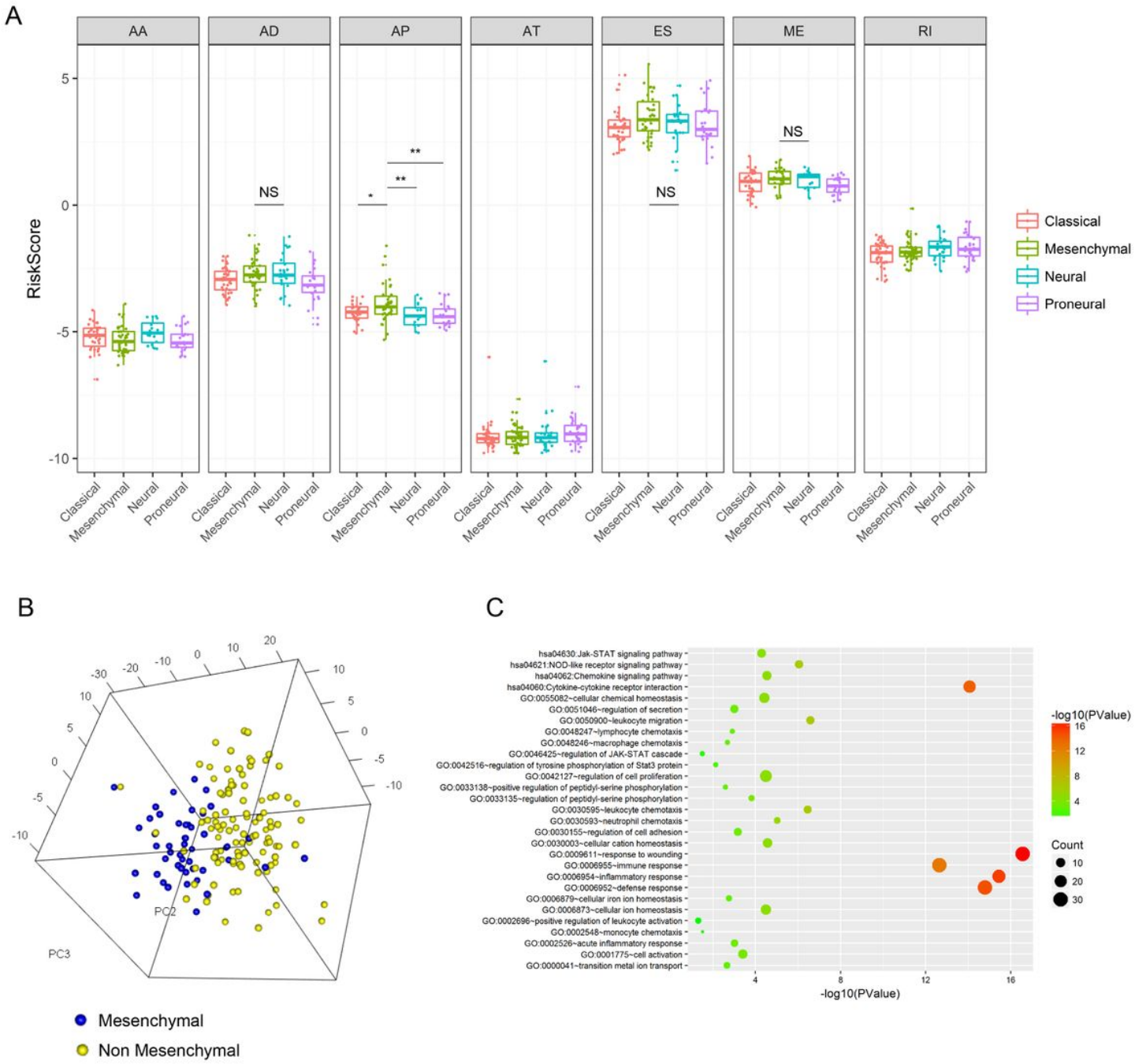

Figure 5

The AP signature was associated with the mesenchymal subtype of GBM. (A) Seven types of AS risk scores were analyzed among four GBM molecular subtypes, and only the AP risk score was significantly elevated in the mesenchymal subtype. (B) PCA analysis showed that mesenchymal samples were distributed with a different pattern than non-mesenchymal samples based on immune-related genes. (C) GO and KEGG analyses were performed based on significantly upregulated genes in the mesenchymal subtype, and the enrichment results showed that the most relevant biological processes were immune-related terms. (*P < 0.05, ** P < 0.01, *** P < 0.001, **** P < 0.0001, NS, not significant)

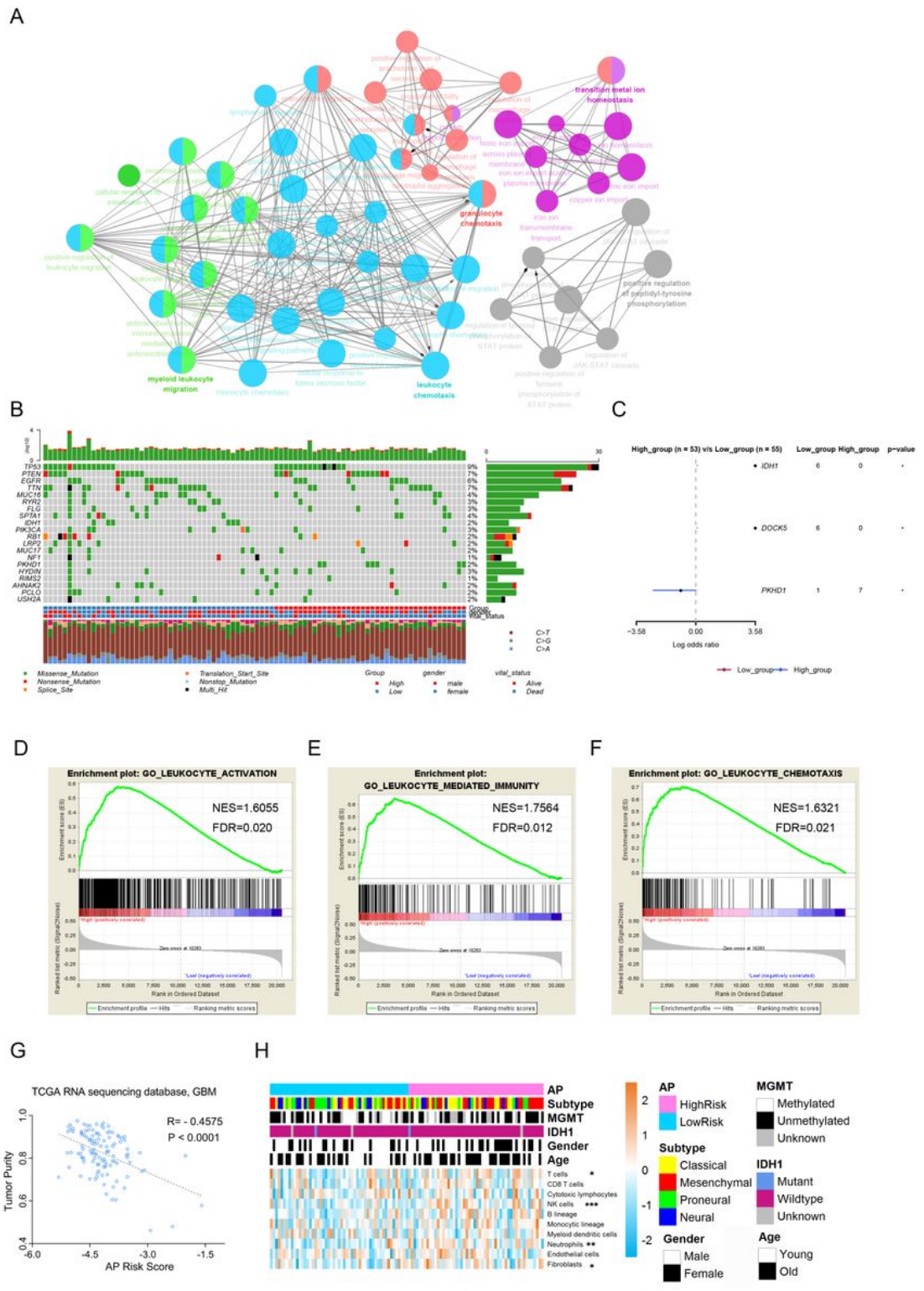

Figure 6

The AP signature was identified as an immune relevant signature. (A) ClueGo analysis showed that the most relevant biological processes related to the AP signature were immune response and immune cell chemotaxis. (B) The exhibition of common somatic mutation events stratified by AP score. (C) Low AP score group occupied more IDH1 mutation. (D-F) GSEA analyses were performed to confirm the ClueGo results. (G) The AP risk score was negatively correlated with GBM purity. (H) MCP results suggested that

neutrophils were the most relevant microenvironment component associated with AP risk. (* P < 0.05, ** P < 0.01, *** P < 0.001, **** P < 0.0001, NS, not significant)

Supplementary Files

This is a list of supplementary files associated with this preprint. Click to download.

- SupplementaryTables.docx